A SECOND FUNDAMENTAL MODEL FOR RESONANCE

J. HENRARD and A. LEMAITRE*

Department of Mathematics, Facultès Universitaires N.D. de la Paix a Namur, B-5000, Namur, Belgium

(Received November, 1982; accepted December, 1982)

Abstract. We analyse a simple one degree of freedom Hamiltonian system depending upon a parameter $H = -3(\delta + 1)R + R^2 - 2\sqrt{2R}\cos r$. This model is much closer to resonance problems arising in Celestial Mechanics than the pendulum.

We deduce from it the conditions of capture into resonance or escape from resonance for systems drifting slowly. We apply this analysis to the Enceladus–Dione resonance.

1. Introduction

The pendulum, the Hamiltonian function of which is

$$H = \frac{a}{2}I^2 - b\cos\phi, \tag{1}$$

has often been taken as the basic model for resonance.

It is the backbone of the so-called *ideal resonance* problem (Garfinkel *et al.*, 1971; see also Jupp 1982 for a more recent contribution). Yoder analyses a version of it with slowly varying parameters (Yoder, 1973, 1979a) and uses it as a pattern after which the evolution of orbit–orbit resonance is described (Yoder, 1973, Peale, 1976).

These references are only a sample. As a matter of fact it would be almost impossible to find a reference about resonances which would not mention the pendulum and which would not use it implicitly or explicitly as a model.

If we look more carefully at the way a resonance problem arising in Celestial Mechanics is reduced to the pendulum (1), we find quite often the following steps.

In a first step, action-angle variables are introduced in such a way that the problem is reduced to a one degree of freedom Hamiltonian system

$$K = K_0(S) + \varepsilon K_1(S, s) \tag{2}$$

where K_1 is 2π-periodic in s (the resonant angle) and $\partial K_0/\partial S$ is small for S close to some value S^*. Without loss of generality, we can take $S^* = 0$.

In a second step, K_0 and K_1 are expanded in Taylor series with respect to S and only the most significant terms are retained.

Here we come to a cross point. In some cases $K_1(0, s)$ is a non constant function of s. Its simplest form is $K_1(0, s) = \cos s$ and we obtain

$$K' = \alpha S + \beta S^2 + \varepsilon\cos s \tag{3}$$

* Supported by the 'Fonds National de la Recherche Scientifique'.

Celestial Mechanics **30** (1983) 197–218. 0008–8714/83/0302–0197 $03.30.

which leads directly to the pendulum (1) after a translation

$$S = I - \alpha/2\beta. \tag{4}$$

But, in many instances in Celestial Mechanics, the function K_1 possesses the d'Alembert characteristic in $(\sqrt{S}, s)$. This means that it is an analytic function in $x = \sqrt{2S}\sin s$ and $y = \sqrt{2S}\cos s$ at the origin (Henrard, 1974).

This is the case in most orbit–orbit resonances where $\sqrt{2S}$ is proportional to the eccentricity or the inclination. This is also the case in many spin-orbit resonances where $\sqrt{2S}$ is proportional to the obliquity (Peale, 1973, Borderies, 1980).

In such cases, the analogous simplest form for the truncated Hamiltonian is

$$K'' = \alpha S + \beta S^2 + \varepsilon\sqrt{2S}\cos s. \tag{5}$$

which corresponds to the strongest resonances (those of the form $p\lambda_1 - (p+1)\lambda_2$, where p is an integer, for satellite–satellite resonances).

Now the relation between the pendulum (1) and (5) is no longer simple.

For some values of the parameters $(\alpha, \beta, \varepsilon)$ and in some limited parts of the phase space (S, s), it is possible to define a non zero mean value $\bar{S}$ of S. Expanding around this mean value, it is possible to compare (5) and (1) with $b = \varepsilon\sqrt{2\bar{S}}$. This is the base of Greenberg's (1977) and Yoder's (1973) work on resonance.

This type of analysis is either incomplete (because it is valid only in a limited part of the phase space and/or the parameter space) or very intricate (because different types of scaling or approximations have to be used in different parts of the phase space and then stitched together).

In view of this, we ask the question: what is gained in the last step, modelling (5) by (1)?

Both of these problems are one degree of freedom problems which can be analysed by mapping the level curves of the Hamiltonian function in the phase space. Of course, most of the computations related to the pendulum can be carried out in terms of elliptic functions which are tabulated and the properties of which are well known.

We feel that this advantage is not important enough to justify the approximations and the intricacies involved in the last step.

Other authors (Schubart, 1966, Message, 1966) have also felt this way. But to stay as close as possible to the physical problem, they went back all the way to Hamiltonian (2), which after all is already a one degree of freedom problem.

But in doing so, each resonance problem is a particular one. We do not have really a model which can be used in many instances. Furthermore, it is not even obvious what problem (2) is. Both Schubart and Message analyse the interior resonance 2/1 in the restricted circular problem. But Schubart defines (2) by a numerical averaging process and thus cannot write down a specific Hamiltonian. On the other hand, Message defines (2) by an expansion in powers of $\sqrt{2S}$. It is not evident that the two formulations are equivalent.

Hence we feel that there is a need for a model between (1) and (2) which would be

almost as simple and as well documented as the pendulum but which would be also closer to the large class of orbit–orbit and spin–orbit resonance problems we have been referring to.

We think that the Hamiltonian (5) is such a model and we like to call it *the second fundamental model of resonance*. The first one being obviously the pendulum.

To make it really a working model, it remains to document it, to describe its solution in a complete and readable form. This is what we would like to do in this paper.

We choose to describe its solution by means of figures rather than tables. This is because we think that an accuracy of a few percent is enough for many applications and because this is more readable. After all, the model will only be an approximation of another problem.

We emphasize also certain aspects of the solution related to the analysis of evolution through resonance by means of the adiabatic invariant. This is because it is in this context that we have felt the necessity of such a model.

2. Scaling the Model

The Hamiltonian (5) depends upon three parameters (α, β, ε). In many applications, β is of the order of unity, α measures the closeness to the resonance and can be vanishingly small, while ε measures the strength of the restoring force and can also be small.

The three parameters are not really independent, and by scaling the time and the action, we can consider that our model has only one truly independent parameter.

Indeed, let us define

$$r = \begin{cases} s \times \operatorname{sign} \beta & \text{if} \quad \beta\varepsilon < 0, \\ s \times \operatorname{sign} \beta + \pi & \text{if} \quad \beta\varepsilon > 0 \end{cases} \tag{6}$$

and the scaled time and momentum

$$\tau = \left| \frac{\beta\varepsilon^2}{4} \right|^{1/3} t, \tag{7}$$

$$R = \left| \frac{2\beta}{\varepsilon} \right|^{2/3} S. \tag{8}$$

The Hamiltonian function (5) is replaced by

$$H(r, R) = -3(\delta + 1)R + R^2 - 2\sqrt{2R} \cos r \tag{9}$$

where δ is the parameter of the model and is given by

$$\delta = -\operatorname{sign}(\alpha, \beta) \times \left| \frac{4}{27} \frac{\alpha^3}{\beta\varepsilon^2} \right|^{1/3} - 1. \tag{10}$$

In the case of orbit–orbit resonance, R is usually proportional to the square of the

eccentricity or the inclination and, in case of spin–orbit resonance, to the square of the obliquity. As ε is usually much smaller than β, the scalings (7) and (8) introduce a slow time τ and an enlarged version of the eccentricity, the inclination, or the obliquity.

The Hamiltonian function (9) is not differentiable at $R = 0$. This is because the coordinates (r, R) are not a regular map of the phase-space at that point and present a *virtual singularity* (Henrard, 1974).

We shall thus introduce the canonical cartesian coordinates

$$y = \sqrt{2R}\,\sin r, \qquad x = \sqrt{2R}\,\cos r \tag{11}$$

where x is the momentum conjugated to y. The Hamiltonian (8) becomes

$$H_2(y, x) = -\tfrac{3}{2}(\delta + 1)(x^2 + y^2) + \tfrac{1}{4}(x^2 + y^2)^2 - 2x \tag{12}$$

and is now regular at the origin.

We shall use (12) rather than (9) whenever the virtual singularity becomes troublesome.

3. Libration and Circulation

The equilibria of the dynamical system (12) are given by the solutions of $\partial H_2/\partial x = \partial H_2/\partial y = 0$. They are thus located at points $(x, y) = (x^*, 0)$ where x^* is a root of

$$x^3 - 3(\delta + 1)x - 2 = 0. \tag{13}$$

For $\delta = 0$, the cubic polynomial (13) has a double root at $x = -1$ and a third root at $x = 2$. For $\delta < 0$, only one root is real, while for $\delta > 0$, the three of them are real. The locations of these roots are given in Figure 1. For $\delta > 0$, one of these equilibria (the leftmost one) is unstable and the other two are stable. Two homoclinic orbits come out of the unstable equilibrium. They enclose one area that we call the *resonance zone* (see Figure 2).

We have to stress here that this definition is not the usual one. Usually resonances are associated with librations: i.e. with orbits along which the angular variable does not take all values between 0 and 2π.

This is perfectly correct for the pendulum where indeed the two concepts coincide. But, in this case, they do not coincide as can be seen from Figures 2 and 3.

In this case the geometrical concept of libration is a poor one: It has no dynamical significance, it depends upon a particular choice of coordinates (the polar coordinates system) and, to make things worse, emphasizes a singularity (the origin) of this coordinate system.

We were tempted to follow Poincaré (1902) and, discarding its geometrical meaning, use the word *libration* as a synonym to resonance. Several of our colleagues have objected to this and indeed this would further the confusion.

Besides the resonance zone, we can distinguish two other zones: an internal zone (inside the smallest homoclinic orbit) and an external zone (outside the largest homoclinic orbit).

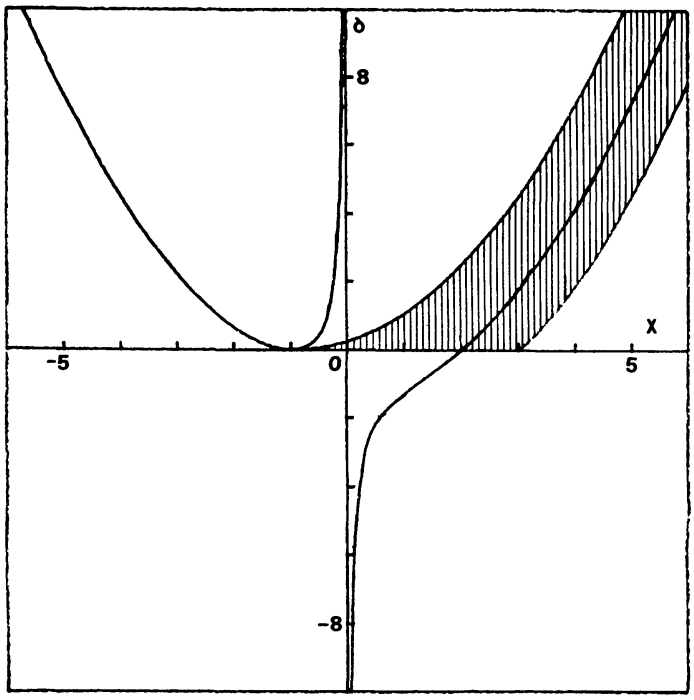

Fig. 1. Location of the equilibria and the resonance zone.

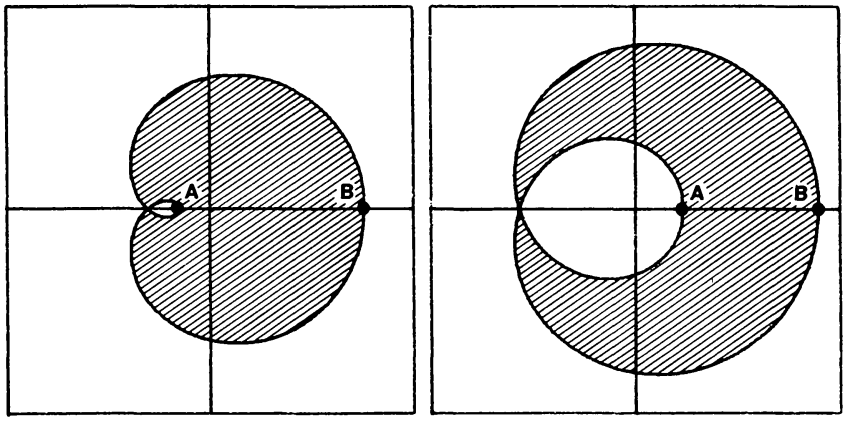

Fig. 2. Resonance Zone.

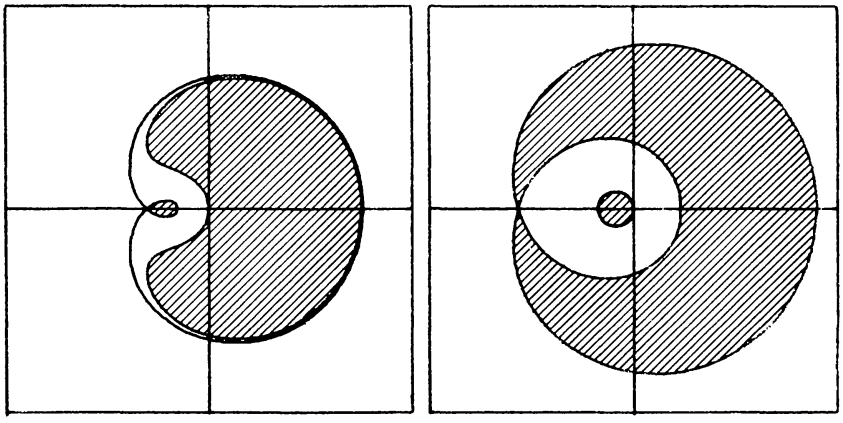

Fig. 3. Libration zones.

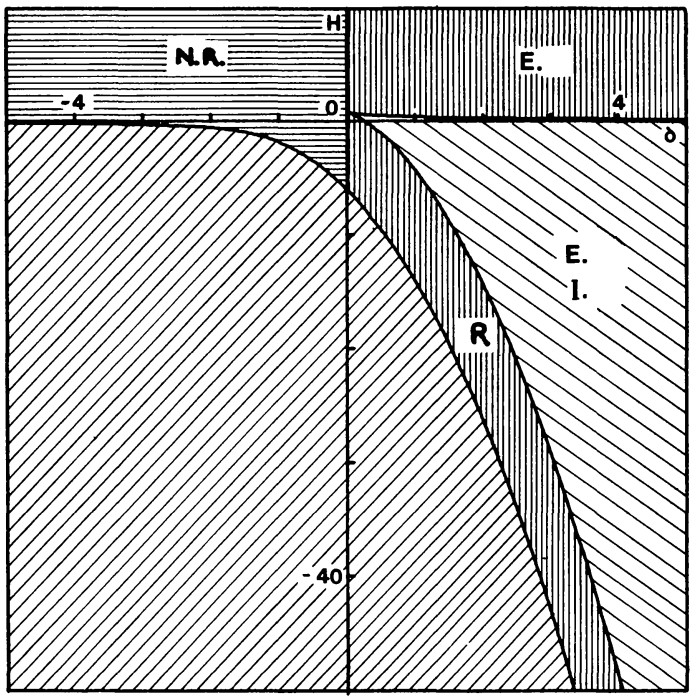

Fig. 4. Types of motion (N. R. : non resonance. (E) external orbits, (I) internal orbits; (R) resonance).

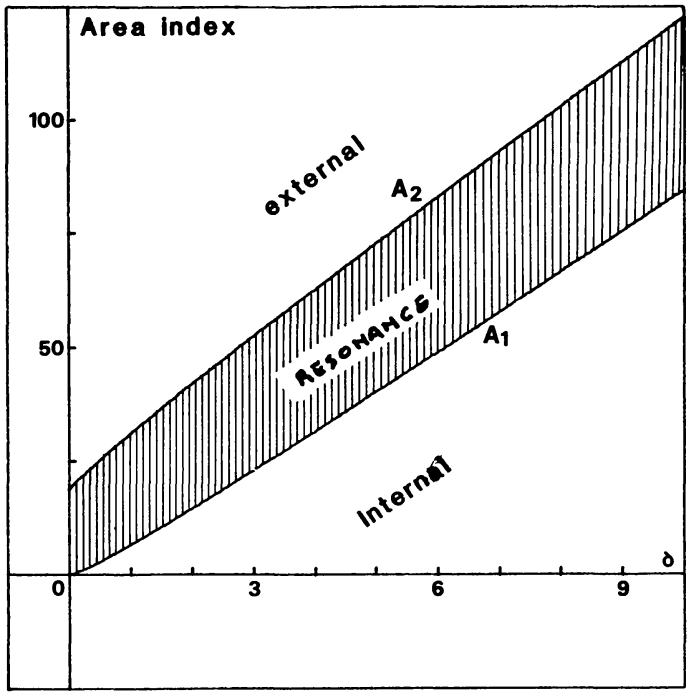

Fig. 5. The critical areas and the zones in the area index diagram.

The location and the importance of these three zones can be read from Figures 1, 4, and 5. In Figure 1, besides the coordinates of the three equilibria, we give the coordinates of the points A and B of Figure 2 and thus the intersections of the three zones with the axis of symmetry.

Figure 4 describes the types of motion in the plane (δ, h) where h is the value of the Hamiltonian function (9) or (12). Figure 5 plots the critical areas A_1 and A_2. They are the areas enclosed by each of the two homoclinic curves.

As we shall see in Section 6, the area enclosed by a trajectory 'γ' is an important quantity to describe evolution through resonance. We shall denote it by $A(\gamma)$ and call it the *area of the trajectory* γ.

We shall also introduce the concept of *Area Index* of a trajectory. For non resonant orbits, it is the same as the area but for resonant orbits, we add to the area of γ, the area enclosed by the smallest of the homoclinic orbits. In this way, there is a one to one correspondence between trajectories and Area Index and the quantities A_1 and A_2 form the boundaries of the three zones.

4. Solution for Moderate δ

In Figures 6 and 7, we have plotted the trajectories of the problem for several values of δ.

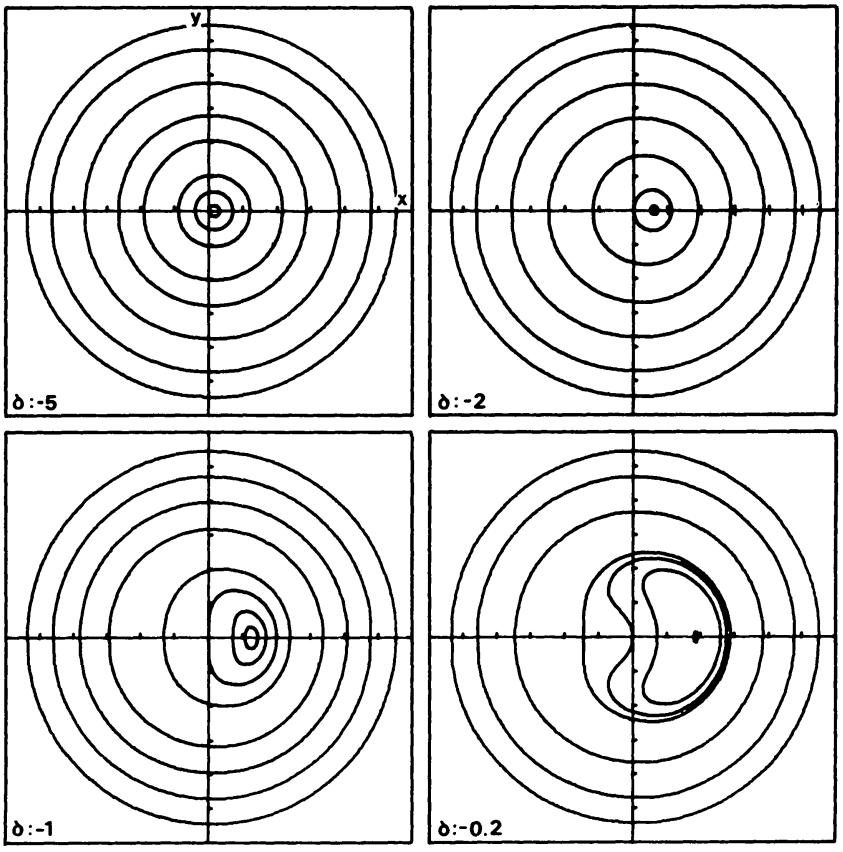

Fig. 6. Trajectories in the plane (x, y) for negative δ.

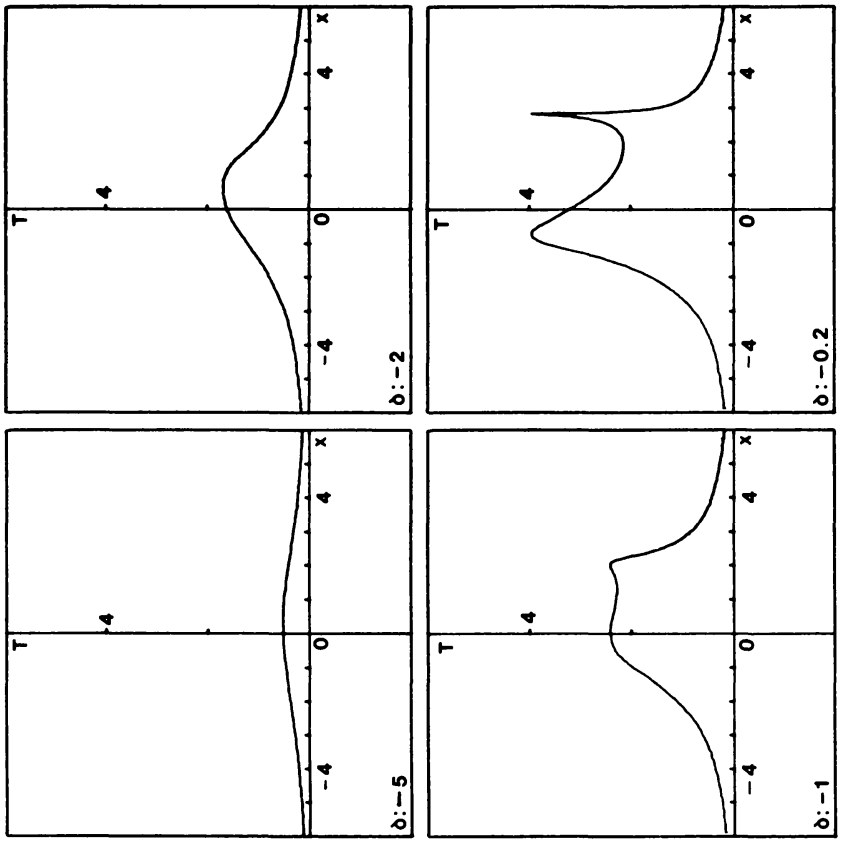

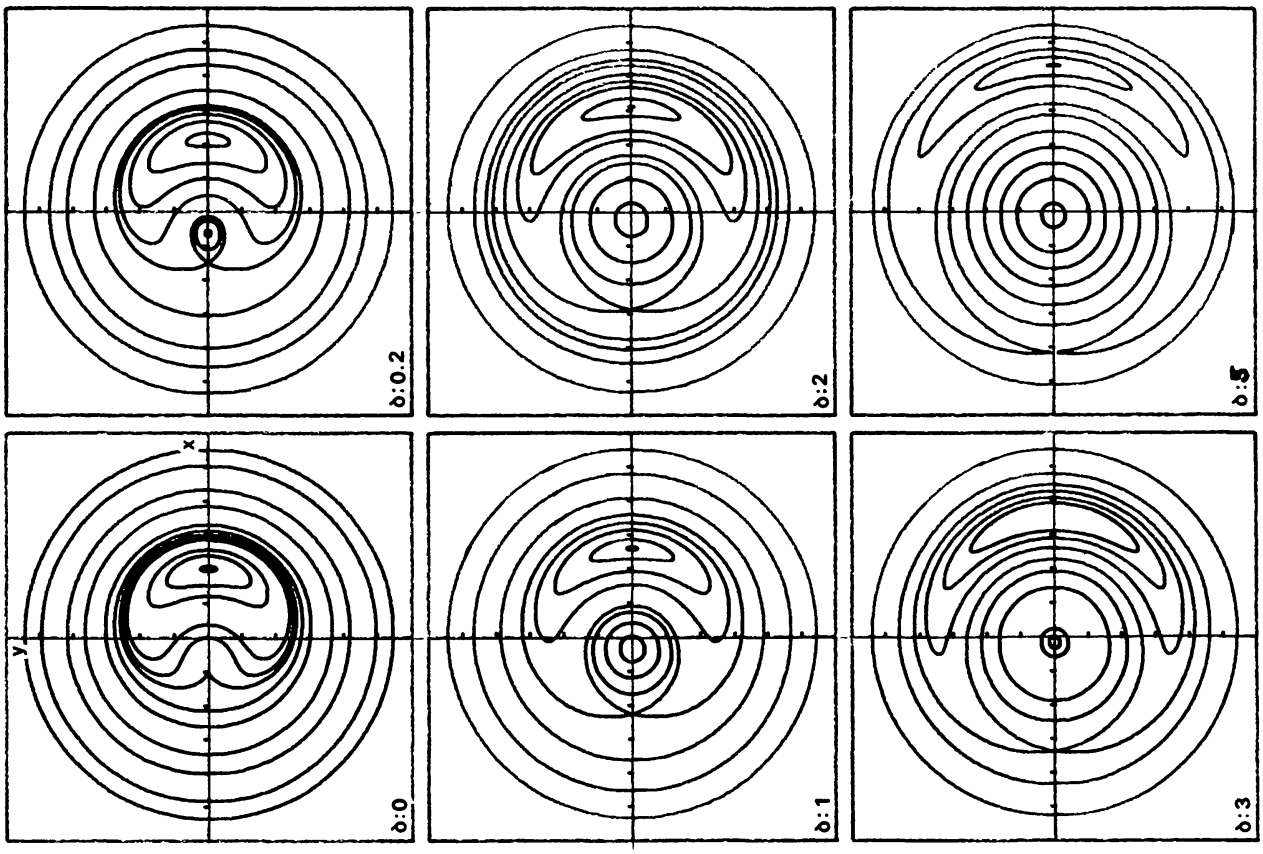

Fig. 8. Period of the trajectories for negative δ.

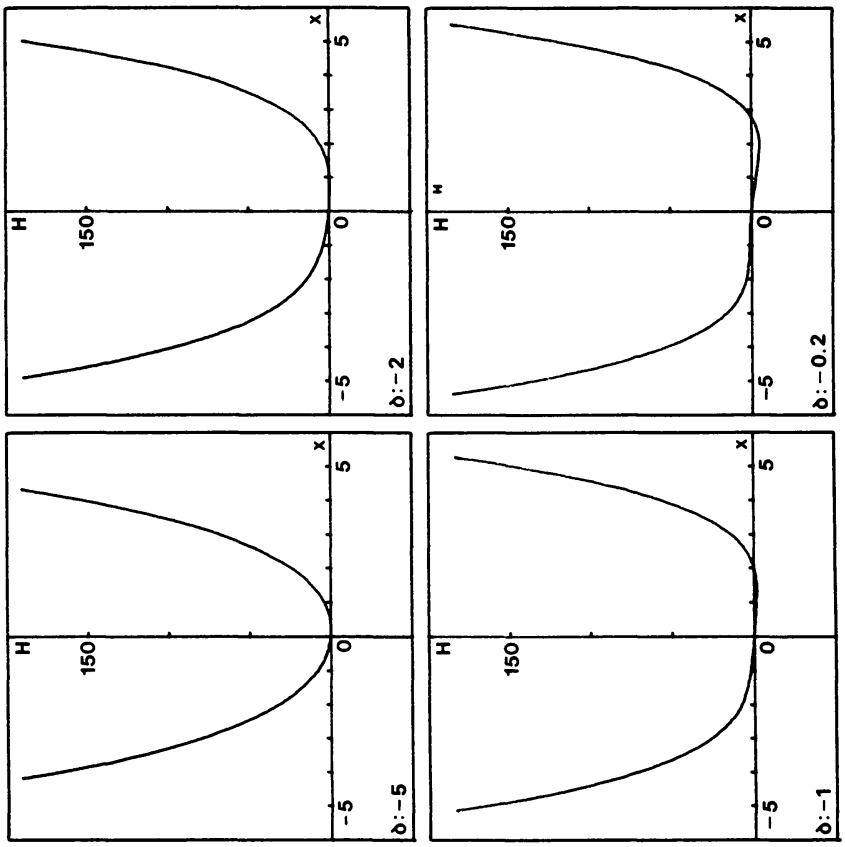

Fig. 10. Energy constants for negative δ.

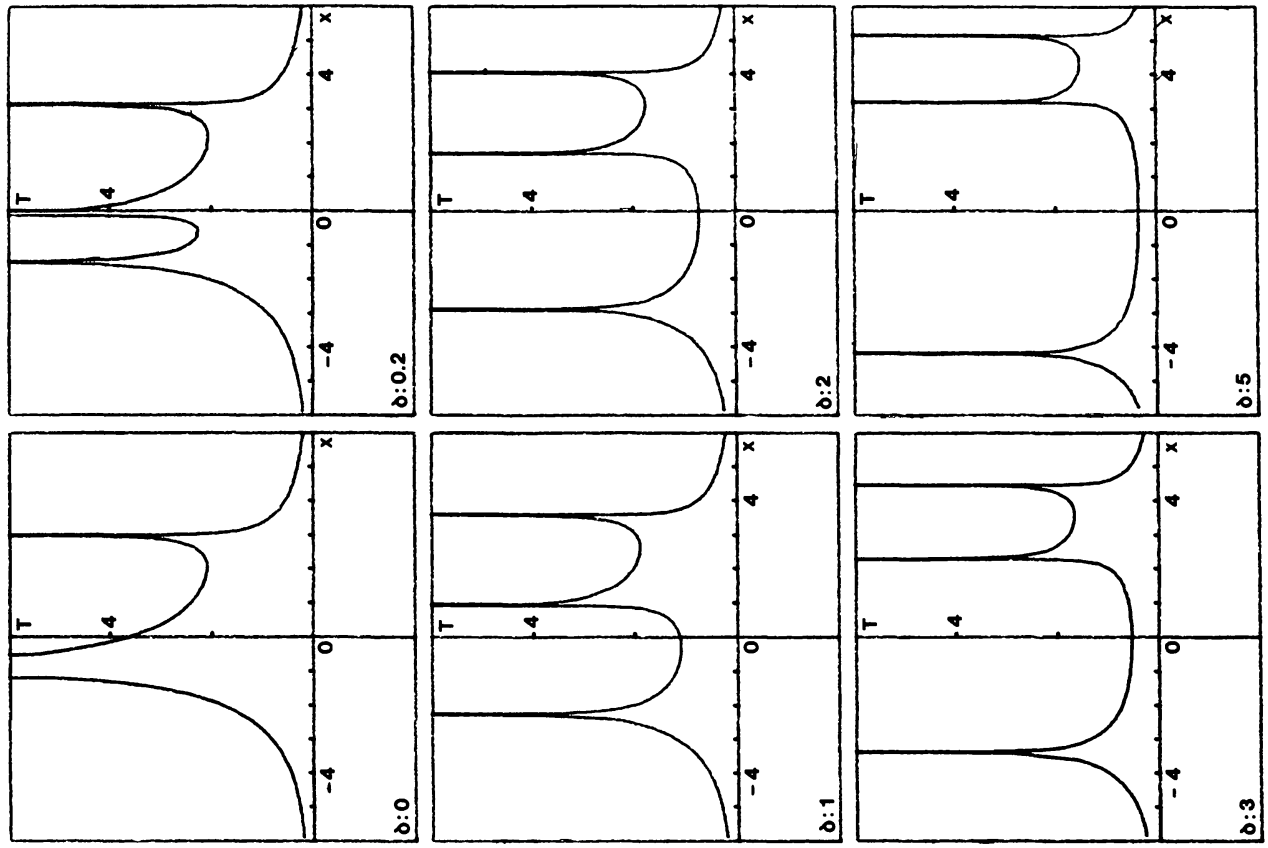

Fig. 9. Period of the trajectories for positive δ.

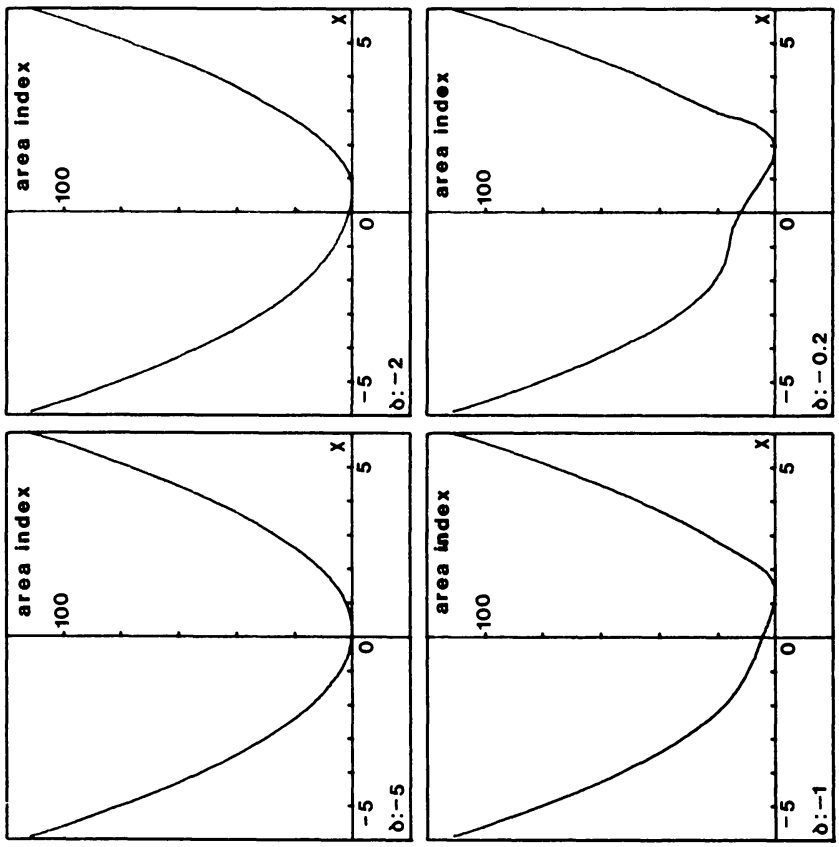

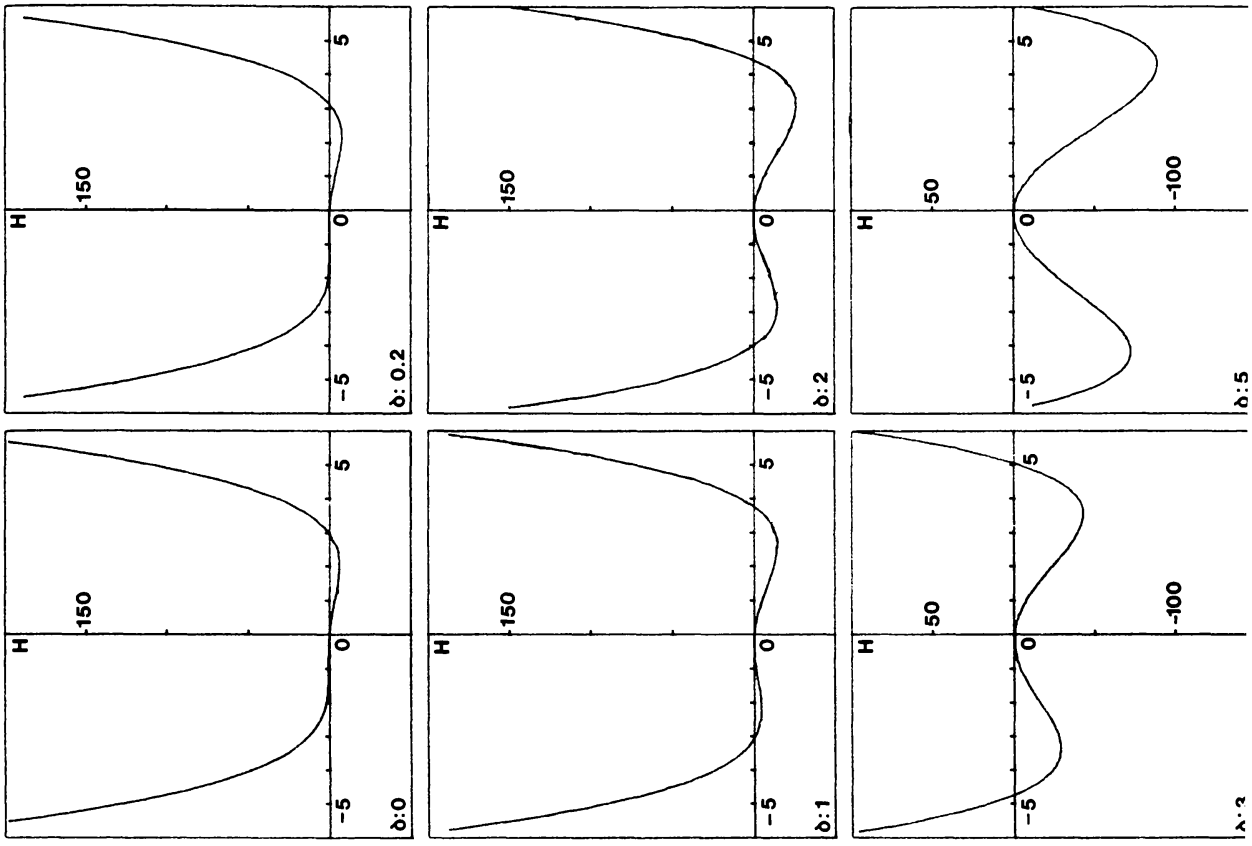

Fig. 12. Area Index for negative δ.

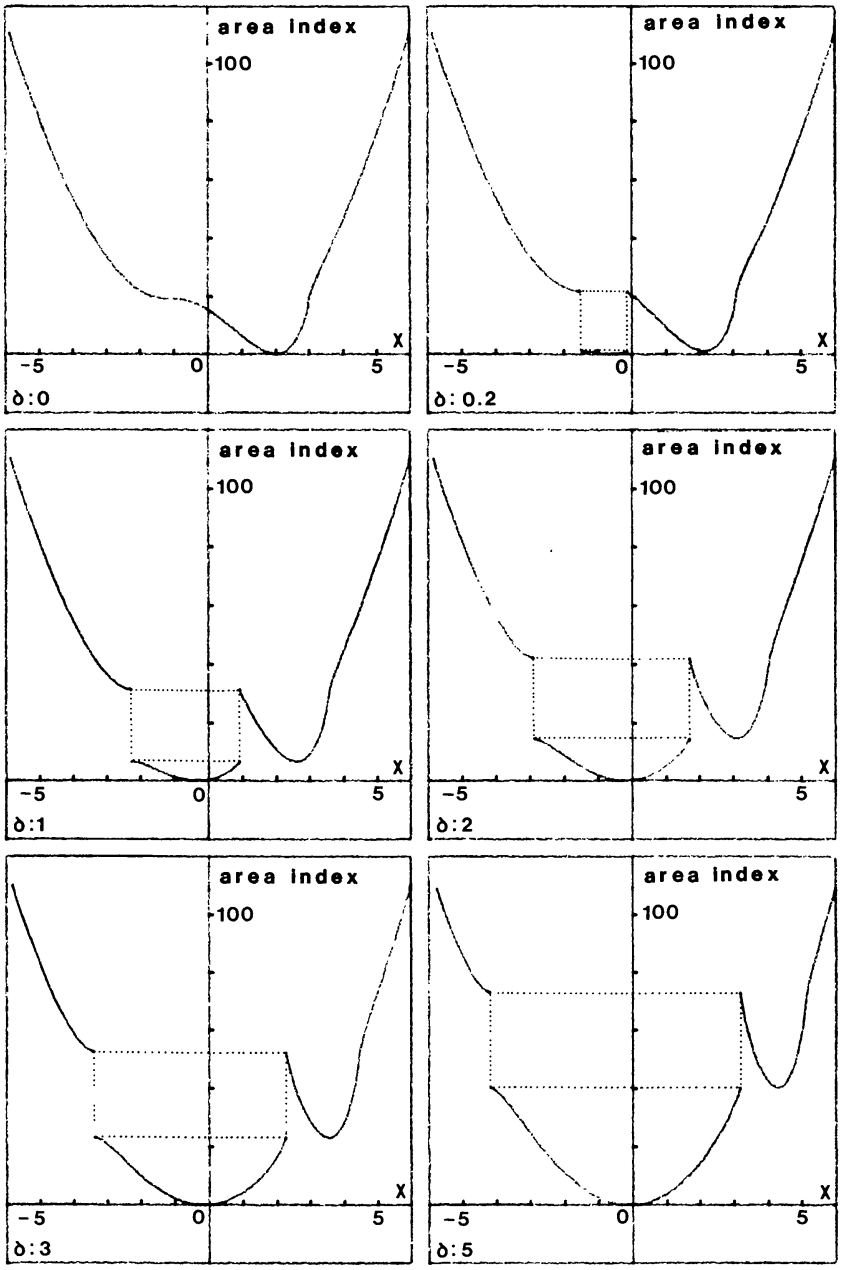

Fig. 13. Area Index for positive δ.

For values of δ larger in absolute value than 5, we are already far enough from the resonance for the approximations for large δ that we describe in the next section to be useful.

For the same values of δ, we give in Figures 8 to 13 other characteristics of the trajectories. We believe that the best way to describe the problem is to plot the values of intrinsic quantities (period, energy constant h, area index) versus the intersection of the trajectories with the axis of symmetry $y = 0$. This intersection is not unique so that each orbit is represented twice in Figures 8 to 13.

It should be possible to read, from Figures 8 to 13, relations between Energy and Period, Energy and Area Index and so on, and at the same time to identify the shape of the corresponding orbits on Figures 6 and 7.

The area index functions (Figures 12 and 13) show a discontinuity for positive δ between internal orbits on one side and external orbits or resonant orbits on the other side. Note however that each trajectory has a different value of the area index.

5. Approximation for Large δ

According to (10), large values of δ correspond physically to a system which is not very close to resonance (α not very small) or to a system with a very weak restoring force (ε very small).

Both situations are of interest. But we have to remember that our model is likely to be a good approximation of a physical problem only if S is small.

This will be true for a large domain (containing the resonance zone) of the phase space (r, R) in the second situation (ε very small) but usually not in the first one. Hence the approximations we are about to develop for large δ will be useful mainly in the case of systems with weak restoring forces.

Most of the quantities of interest (that we have computed numerically and plotted in the case of moderate δ) can be expressed analytically in negative power series of δ for large values of this parameter.

We shall develop in this section the first few terms of these expansions. They supplement the figures of Sections 3 and 4 to give a picture of the solution of our fundamental model for all values of δ.

Let us define

$$\Delta = 3(\delta + 1). \tag{14}$$

It is easily checked that, for large values of δ, the three singular points of the problem can be approximated by

$$x_1 = -\Delta^{1/2}\{1 - \Delta^{-3/2} - \tfrac{3}{2}\Delta^{-3}\} + O(\Delta^{-4}), \tag{15}$$

$$x_2 = -2\Delta^{-1}\{1 + 4\Delta^{-3}\} + O(\Delta^{-5}), \tag{16}$$

$$x_3 = \Delta^{1/2}\{1 + \Delta^{-3/2} - \tfrac{3}{2}\Delta^{-3}\} + O(\Delta^{-4}). \tag{17}$$

Of course, when $\Delta < 0$, only the second equilibrium point (close to the origin) is real.

The resonance zone (when $\Delta > 0$) encircles the third equilibrium point (which is stable). The homoclinic curves which form its boundaries are given by

$$R_c = \frac{\Delta}{2} \pm 2\Delta^{1/4} \cos\frac{r}{2} + \Delta^{-1/2} \cos r + O(\Delta^{-5/4}). \tag{18}$$

They have a singular point at the location of the first equilibrium ($r = \pi$).

From (18), we deduce approximations for the smallest (A_1) and largest (A_2) critical

areas:

$$A_1 = \pi\Delta - 8\Delta^{1/4} + O(\Delta^{-5/4}), \tag{19}$$

$$A_2 = \pi\Delta + 8\Delta^{1/4} + O(\Delta^{-5/4}). \tag{20}$$

Hence the area of the resonance zone is

$$A_L = 16\Delta^{1/4} + O(\Delta^{-5/4}). \tag{21}$$

In most of the non resonance domains (internal as well as external), the graphs in Section 4 can be extended by the following formulae.

Let us define

$$\rho = [4h + \Delta^2]^{1/2} \tag{22}$$

where h is the value of the Hamiltonian function (9).

When ρ is larger than $\Delta^{1/4}$, we have that the curves $H = h$ are given by

$$\begin{cases} x = \pm\dfrac{2}{\rho} + [\Delta \pm \rho]^{1/2}\cos r \mp 4\dfrac{[\Delta \pm \rho]^{1/2}}{\rho^3}\cos^3 r + \cdots, \\ \\ y = [\Delta \pm \rho]^{1/2}\sin r \mp 4\dfrac{[\Delta \pm \rho]^{1/2}}{\rho^3}\cos^2 r \sin r + \cdots. \end{cases} \tag{23}$$

When $4h < -\Delta^2$, there are no level curves because ρ is not real. When $-\Delta^2 < 4h < 0$, there are two level curves corresponding to the two signs in (23). When $4h > 0$, there is only one curve because $\Delta - \rho < 0$.

If we neglect the last terms in (23), which are in any case smaller than $\Delta^{-1/4}$, the level curves are circles in the plane (x, y) with radius $[\Delta \pm \rho]^{1/2}$.

Leading terms in the expansions of the area and the period of a trajectory can be easily deduced. We find

$$A = \pi[\Delta \pm \rho] + \cdots, \tag{24}$$

$$T = 2\pi/\rho + \cdots. \tag{25}$$

At the internal equilibrium x_2, h is almost zero and the period is then given by $T = 2\pi/\Delta$. In the original time unit, before normalization, this is equal to $2\pi/\alpha$ as could be expected.

In the resonance zone, the solution can be approximated by the simple pendulum. Indeed, if we make the translation

$$R = \frac{\Delta}{2} + I, \tag{26}$$

the Hamiltonian function (9) becomes

$$k = \tfrac{1}{8}(4h + \Delta^2) = \tfrac{1}{2}I^2 - \Delta^{1/2}\cos r + O(\Delta^{-1/2}). \tag{27}$$

The period, the area and the energy can thus be approximated by

$$T \simeq 4\Delta^{-1/4}\,\mathbb{K}(\lambda), \tag{28}$$

$$A \simeq 16\Delta^{1/4}\{(\lambda-1)\mathbb{K}(\lambda)+\mathbb{E}(\lambda)\}, \tag{29}$$

$$h \simeq -\frac{\Delta^2}{4}+2\Delta^{1/2}(2\lambda-1) \tag{30}$$

where $\mathbb{K}(\lambda)$ and $\mathbb{E}(\lambda)$ are the complete elliptic integrals and the modulus λ is related to the maximum elongation of the solution

$$\lambda = \sin^2\frac{r_{\max}}{2}. \tag{31}$$

The maximum value of I, corresponding to $r = 0$, is given by

$$I_{\max} \simeq 2\Delta^{1/4}\lambda^{1/2}. \tag{32}$$

6. Evolution through Resonance

Let us assume that the parameter δ varies slowly with the time, i.e.

$$|\dot{\delta}| \leqslant \eta, \qquad |\ddot{\delta}| \leqslant \eta^2, \tag{33}$$

where η is some small quantity. The solutions of system (9) are no longer the closed curves described in the previous section but they are close to them.

More specifically, the solutions of system (9) with varying δ stay for a moderate amount of time within η of a solution of system (9) with constant δ (which we shall call the *guiding solution*).

In the long run, the guiding solution evolves. To identify it, we use the theory of the adiabatic invariant (see, for instance, Henrard, 1982b); it states that the area enclosed by the guiding trajectory does not change by more than η, for an evolution of the system limited to times smaller than η^{-1}.

It may happen that the guiding trajectory becomes an homoclinic orbit at some point in the evolution. In that case, the classical theory of the adiabatic invariant breaks down. We have shown (Henrard, 1982a) that under some assumptions (which are verified by system (9)), the evolution of the system can be described in the following terms.

Let us assume that the guiding trajectory is first a non resonant trajectory (external or internal). After going through an homoclinic orbit, it may become either a non resonant trajectory of the other type or a resonant trajectory. Whether it becomes one or the other depends on the phase at the time of transition and is best expressed in terms of probability assuming that all phases are equally probable.

In both cases, the area enclosed by the guiding trajectory undergoes a discontinuity at the transition but then stays constant again.

Let us apply those principles to our model. Let us first investigate the case when δ decreases with the time.

The guiding trajectory is most likely to be an internal because, in the past, when δ was very large, the other types of trajectories were very far away in the phase space, for large values of R. We thus restrict our analysis to this case.

When δ decreases through zero, the area of the largest possible internal orbit goes to zero. Hence the guiding trajectory is forced to undergo a transition and to become an external. No capture into resonance is possible because the area of the resonant zone is also decreasing with δ (see Figure 5).

The transition imposes a discontinuity in the area index of the guiding trajectory. We choose to represent it in Figure 14 in terms of what we call the *amplitude of the free vibration*

$$F = \left[\frac{\text{Area}}{\pi}\right]^{1/2}. \tag{34}$$

This is based upon the following consideration. When δ is large in absolute value (a long time before or after the transition), the trajectory is almost a circle with F as radius and the origin as center.

In case of orbit–orbit resonance, F can then be interpreted as a normalized (by the normalization (8)) eccentricity or inclination. For spin–orbit resonance, it is a normalized obliquity.

In Figure 14, we have plotted the final value of this quantity F_f with respect to its initial value F_i. Figure 14 can be completed for large values of F_i by the following

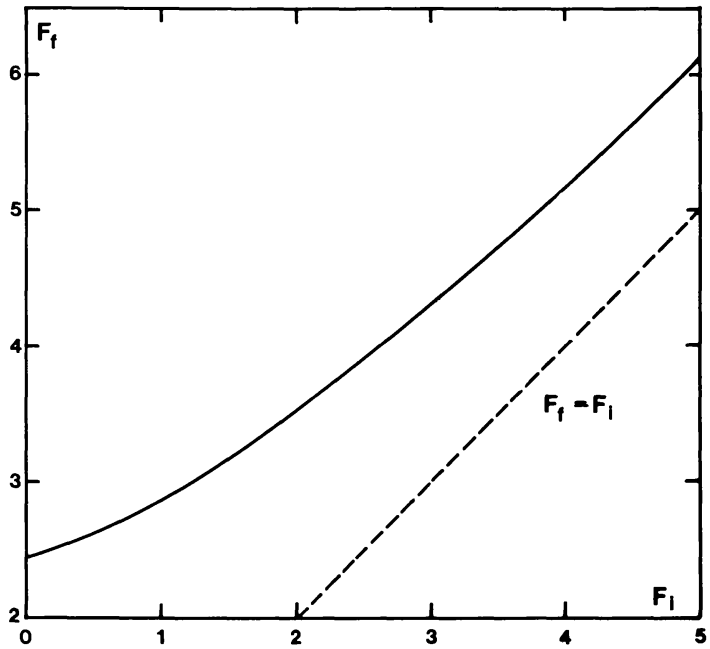

Fig. 14. The amplitude of the free vibration after transition (F_f) versus its value (F_i) before transition for a passage through resonance with decreasing δ.

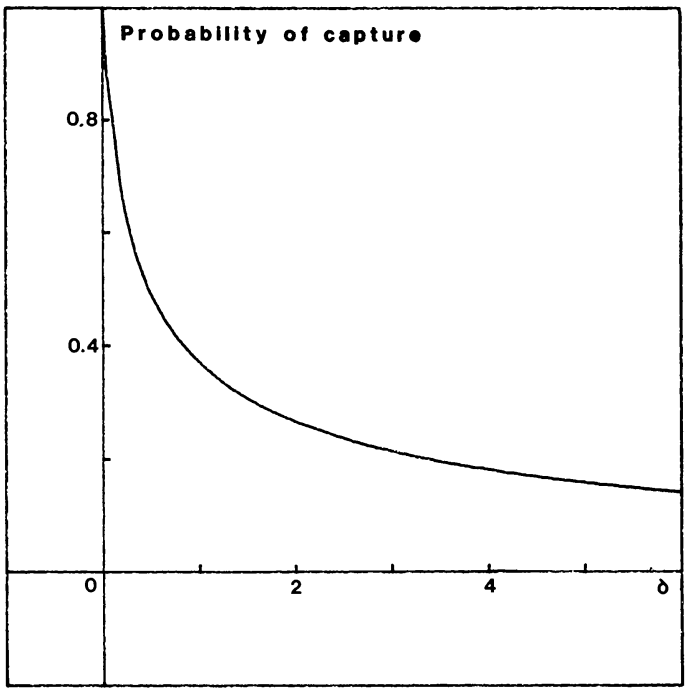

Fig. 15. Probability of capture into resonance when δ increases.

approximation

$$F_f \simeq F_i + \frac{8}{\pi} F_i^{-1/2}. \tag{35}$$

Let us now turn to the other case of evolution, when δ increases with time. In the past, δ was negative and there is only one type of trajectory: non resonance. When δ reaches zero, an homoclinic trajectory appears and some of these trajectories (those corresponding to an amplitude of free vibration F_i smaller than 2.45) become resonance. This change is done without transition through an homoclinic orbit. The other trajectories become external.

As the area enclosed by the external homoclinic orbit grows without bound with δ, the external guiding trajectories will sooner or later undergo a transition. They can become resonant or internal.

We show, in Figure 15, the probability that they become resonant. For large values of F_i, this probability is small and can be approximated by

$$P_c \simeq \frac{4}{\pi} F_i^{-3/2} \quad . \tag{36}$$

In Figure 16, we give the amplitude of the free vibration after transition (F_f) versus its value before transition (F_i). The jump is always negative. In case of escape, it can be again interpreted as a jump in the normalized eccentricity inclination or obliquity.

In the case of capture into resonance, this amplitude is not very informative on the

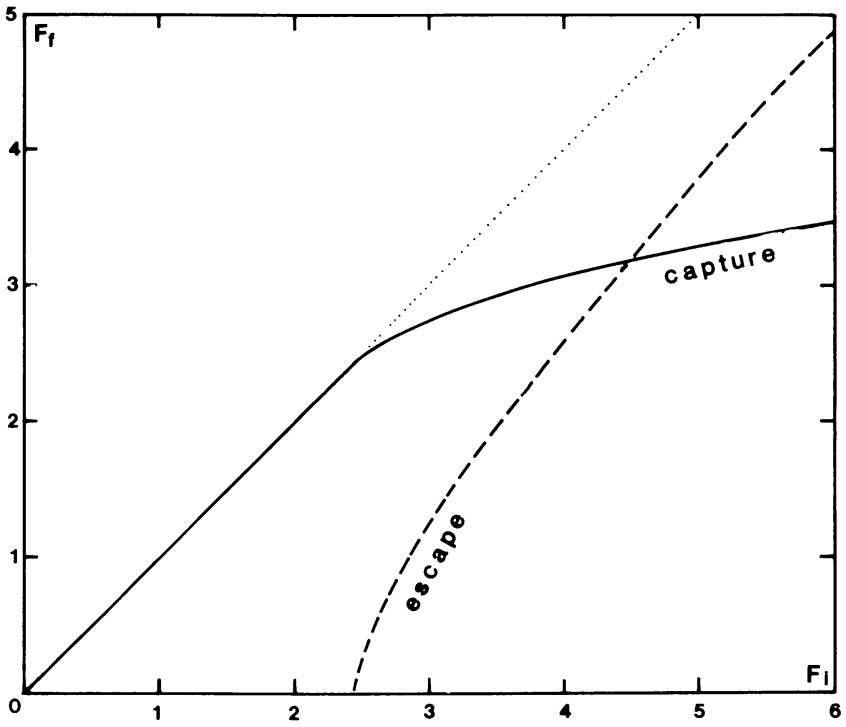

Fig. 16. Amplitude of the free vibration after transition (F_f) versus its value before transition (F_i) for a passage through resonance with increasing δ.

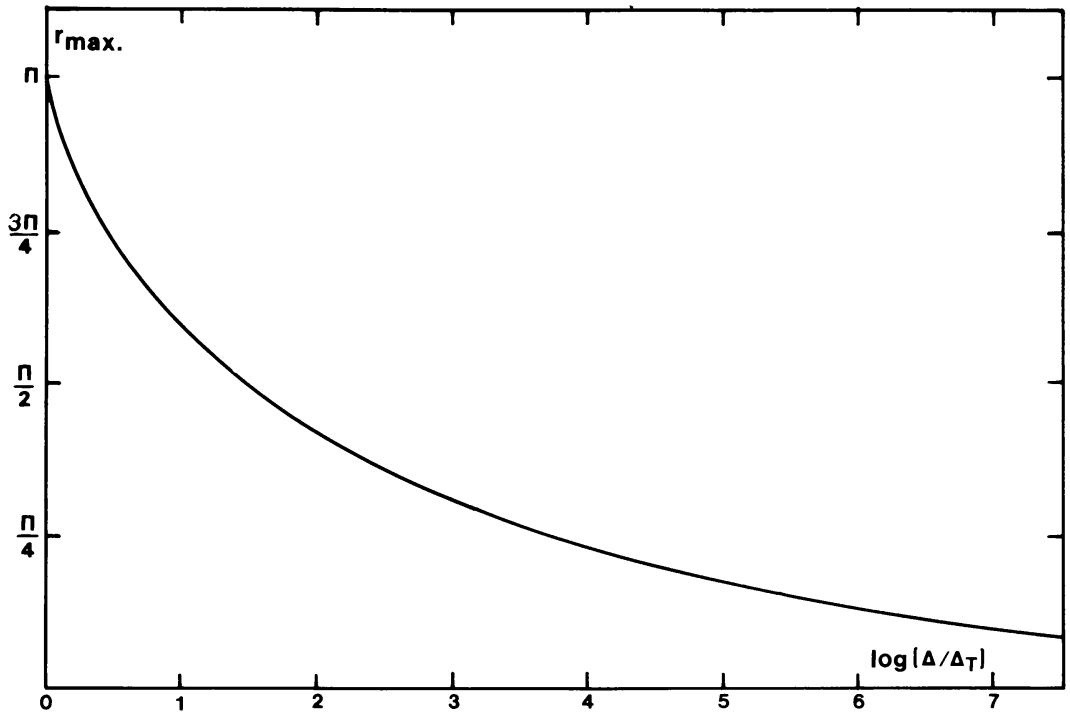

Fig. 17. Amplitude of libration after transition from external to resonant orbit (Δ_T is the value of Δ at transition).

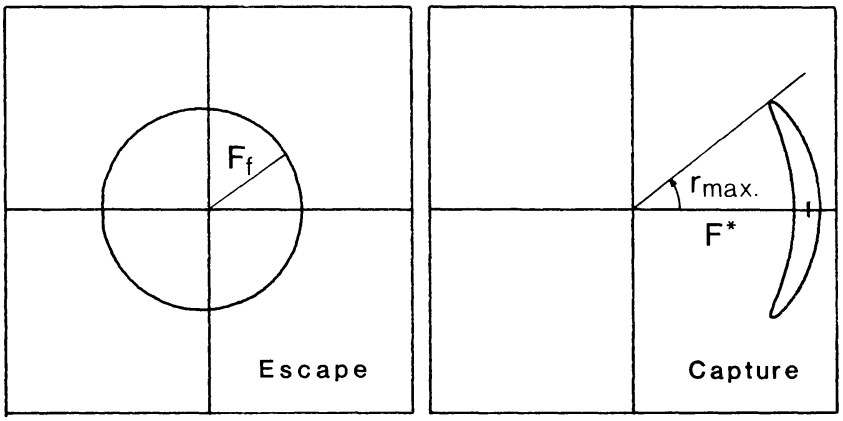

Fig. 18. Guiding trajectory after transition.

final state of the motion because the trajectories do not approach circles for large values of δ. A better way to describe the evolution of the guiding trajectory is in terms of the *forced vibration* F^* defined as the coordinate of the resonant equilibrium and plotted in Figure 1. This quantity does not depend upon the initial state F_i but only upon the value of δ.

Another informative quantity is the amplitude of the libration of the angular variable r. This amplitude decreases slowly with increasing δ. Asymptotically we have

$$r_{\max} = \left(\frac{16}{\pi}\right)^{1/2} (\Delta_T/\Delta)^{1/8} \tag{37}$$

where Δ_T is the value of Δ at the time of transition. For large values of the initial free vibration F_i, it is approximatively equal to F_i^2.

For moderate values of F_i and Δ_T/Δ, this amplitude can be deduced from Figure 17. The values of F_f in function of F_i can be read from Figure 16. Figure 18 shows how the free vibration, forced vibration and amplitude of libration can be used to describe the shape of the trajectory after transition.

7. An Application to Enceladus-Dione

Three resonant pairs of satellites of Saturn: Mimas–Thetys, Enceladus–Dione and Titan–Hyperion have received much attention. Possible scenario of capture into resonance have been analysed numerically (Sinclair, 1972–1974; Greenberg, 1973; Colombo *et al.*, 1974) or analytically (Goldreich, 1965; Yoder, 1973; Peale, 1976).

The fundamental model for resonance we have just described is well suited for such an analysis. We shall apply it in this section to the case of the resonance Enceladus–Dione where we can add a new feature of scenario: the near capture into a resonance involving the perigee of Dione rather than Enceladus.

As a model of the 2–1 resonance Enceladus–Dione, we take the planar planetary

three body problem. We truncate the perturbation function after the first power in the mass ratios satellites/planets and we retain only the long period terms at the first order in the eccentricities. The Hamiltonian function is thus (see Henrard, 1982c)

$$H_{TB} = -\frac{Gm_0m_1}{2a_1} - \frac{Gm_0m_2}{2a_2} - \\ -\frac{Gm_1m_2}{a_2}\{-1.190e_1\cos(\lambda_1 - 2\lambda_2 - p_1) + \\ + 0.428e_2\cos(\lambda_1 - 2\lambda_2 - p_2)\} \tag{38}$$

where the indices 0, 1, 2 refer respectively to Saturn, Enceladus, and Dione. The semi-major axis (a_i) and eccentricities (e_i) are related to the momenta L_i, P_i by the approximate formulae

$$L_i = m_i\sqrt{Gm_0a_i}, \qquad P_i = \tfrac{1}{2}L_i e_i^2. \tag{39}$$

The angular variables conjugated to these momenta are the mean longitudes $\lambda_i = l_i + g_i$ and the opposite of the arguments of perigee $p_i = -g_i$.

To the Hamiltonian (38), we add the secular terms of the effect of Saturn's oblateness

$$H_{\text{ob}} = -\frac{1}{2}J_2\left(\frac{R_S}{a_1}\right)\frac{n_1L_1}{\left(1-\frac{P_1}{L_1}\right)^3} - \frac{1}{2}J_2\left(\frac{R_S}{a_2}\right)\frac{n_2L_2}{\left(1-\frac{P_2}{L_2}\right)^3} \tag{40}$$

where R_S is the equatorial radius of Saturn.

We perform a canonical change of variables to bring forward the two resonant angles

$$\begin{cases} q_1 = p_1 - \lambda_1 + 2\lambda_2, & Q_1 = P_1, \\ q_2 = p_2 - \lambda_1 + 2\lambda_2, & Q_2 = P_2, \\ q_3 = \lambda_1, & L_1 = Q_3 - Q_1 - Q_2, \\ q_4 = \lambda_2, & L_2 = Q_4 + 2Q_1 + 2Q_2. \end{cases} \tag{41}$$

We expand the secular part of the Hamiltonian $H = H_{TB} + H_{\text{ob}}$ in powers of Q_1, Q_2 retaining only the first two orders and we evaluate the coefficients for $m_1/m_0 = 1.27 \times 10^{-7}$, $m_2/m_0 = 1.8 \times 10^{-6}$, $n_1/n_2 \simeq 2$. We find

$$\frac{1}{n_1}H = b_1Q_1 + b_2Q_2 - 1.668(Q_1+Q_2)^2/L_1 + \\ + \sqrt{L_1}\{1.349 \times 10^{-6}\sqrt{2Q_1}\cos q_1 - 1.148 \times 10^{-7}\sqrt{2Q_2}\cos q_2\} \tag{42}$$

where

$$b_1 = 2\frac{n_2^*}{n_1^*} - 1 - 1.589 \times 10^{-3}, \qquad b_2 = 2\frac{n_2^*}{n_1^*} - 1 - 3.166 \times 10^{-4}. \tag{43}$$

The quantities n_1^*, n_2^* depend upon the constants of the motions Q_3 and Q_4. They represent the mean motions of λ_1 and λ_2 when $Q_1 = Q_2 = 0$.

The tides raised upon Saturn by the satellites will have for effect to change slowly the values of Q_3 and Q_4 and thus the values of n_1^* and n_2^*. We have

$$\frac{\mathrm{d}}{\mathrm{d}t}\left(\frac{n_2^*}{n_1^*}\right) = 0.869 \times 10^{-11}\frac{k_S}{Q_S} n_1^* \simeq 0.6 \times 10^{-16} n_1^* \tag{44}$$

where k_S is the Love number ($k_S \simeq 0.34$) and Q_S the tidal dissipation factor ($Q_S \simeq 5.10^4$) of Saturn (see, for instance, Yoder and Peale, 1981).

As the ratio n_1^*/n_2^* drifts slowly, both of the arguments q_1 and q_2 can enter into resonance but not simultaneously because the effect of Saturn's oblateness (responsible for the terms 1.589×10^{-3} and 3.166×10^{-4} in the coefficients b_1 and b_2) is large enough to separate them.

As n_2^*/n_1^* grows slowly, the first resonance to be encountered is the one involving q_2. When b_2 is small enough, b_1 is large enough that the angular variable q_1 can be averaged out of (42) and the Hamiltonian to be considered is

$$H = n_1\{b_2 Q_2 - 1.668\, Q_2^2/L_1 - 1.148 \times 10^{-7}\sqrt{2L_1 Q_2}\cos q_2\}. \tag{45}$$

This Hamiltonian is replaced by our model Hamiltonian (9) by the scaling (see Equations (7), (8), (10))

$$e_2 = \sqrt{2Q_2/L_2} = 7.697 \times 10^{-4}\sqrt{2R}, \tag{46a}$$

$$n_1 t = 5.67 \times 10^4 \tau, \tag{46b}$$

$$\delta = 1.89 \times 10^4 b_2 - 1. \tag{46c}$$

Obviously, Dione has escaped the capture into this resonance. Its present free eccentricity of 2.2×10^{-3} corresponds by the scaling (46) to a free vibration $F_f = 2.86$. According to Figure 20, this corresponds to a value $F_i = 4.2$ of the free vibration before transition and thus by scaling to a free eccentricity of 3.23×10^{-3}. The probability of escape is read from Figure 19. It is $P_{\text{escape}} = 80\%$.

From Figure 6, we find that transition has occurred for $\delta = 3.33$ i.e. for $b_2 = 2.291 \times 10^{-4}$. For these values, we have $A_2 = \pi F_i^2$ and $A_1 = \pi F_f^2$.

Taking into account the present value of $2n_2^*/n_1^* - 1 = 1.315 \times 10^{-3}$ (we shall deduce it from the other resonance), we find that the present value of δ is 17.87 and thus that transition has occured $2.64 \times 10^4 Q_S/k_S \simeq 3.9 \times 10^9$ years ago. Of course, this time scale is very much uncertain as Q_S is. In any case, it should be corrected by taking into account the tides raised on Dione by Saturn.

The effect of these tides on the eccentricity is given by (see Peale *et al.*, 1980)

$$\dot{e}_2 = -\frac{21}{2}\frac{k_2}{Q_2}\left(\frac{R_i}{a}\right)^5\left(\frac{m_0}{m_i}\right)n_2 e_2 = -3.53\times 10^{-5}\frac{k_2}{Q_2}e_2 \text{ per year}$$

where R_2 is the radius of Dione, k_2 its Love number and Q_2 its dissipation factor. This linear equation gives also the variation of F with the time. Replacing the time by differences in values of δ by means of (43), (44) and (46c), we find

$$F_{tr} = 2.86 \exp\left\{+642\times 10^{-2}\frac{Q_S}{Q_2}\frac{k_2}{k_S}(\delta_{now}-\delta_{tr})\right\}. \tag{47}$$

Using likely values, $Q_S = 5.10^4$, $k_S = 0.34$, $Q_2 = 100$, $k_2 = 5.10^{-4}$, we find that transition (when $\pi F_{tr}^2 = A_1$) took place when $\delta = 7.9$, i.e. 2.7×10^9 years ago.

The other resonance involving the angle q_1 (and thus the perigee of Enceladus) is the one that has been investigated by previous authors. Its is described by the Hamiltonian

$$H = n_1\{b_1 Q_1 - 1.668 Q_1^2/L_1 + 1.349\times 10^{-6}\sqrt{2L_1Q_1}\cos q_1\}. \tag{48}$$

The scaling

$$e_1 = \sqrt{2Q_1/L_1} = 7.395\times 10^{-3}\sqrt{2R}, \tag{49a}$$

$$\eta_1 t = 1.096\times 10^4 \tau, \tag{49b}$$

$$\delta = 0.365\times 10^4 b_1 - 1 \tag{49c}$$

reduces it to our non dimensional Hamiltonian (9).

The present state of the motion is characterized by a small libration of the angular variable q_1 (about 1° of amplitude) and a forced eccentricity of 4.45×10^{-3}.

The forced eccentricity when scaled according to (49), means an equilibrium at $-\sqrt{2R}\cos q_1 = x = -0.602$. We read from Figure 2 that δ is thus equal to -2. (We deduce from this the present value of $2n_2^*/n_1^* - 1$ used earlier). Hence we are not yet in a true resonance as defined in Section 2 but only in an apparent libration due to the smallness of the free eccentricity.

For this value of δ, the curves in the plane (x, y) are very well approximated by circles around the equilibrium. The amplitude of the libration of q_1 can thus easily be translated in terms of free eccentricity

$$e_{free} = e_{forced}\cdot\sin 1^\circ \simeq 7.8\times 10^{-5}. \tag{50}$$

The free eccentricity seems to be small. But we ought to consider that it has been damped by tides raised upon Enceladus. The mechanism of this damping is more involved than the one described for Dione because Enceladus is locked in resonance and we shall not attempt to analyse it here.

References

Borderies, N.: 1980, 'La rotation de Mars: Théorie analytique, Analyse d'observations de l'expérience Viking', Thesis, Univ. P. Sabatier (Toulouse).
Colombo, G., Franklin, F. A., and Shapiro, I. I.: 1974, *Astron. J.* **79**, 61.
Garfinkel, B., Jupp, A., Williams, C.: 1971, *Astron. J.* **76**, 157.
Greenberg, R.: 1973, *Astron. J.* **78**, 338.
Greenberg, R.: 1977, *Vistas in Astronomy* **21**, 209.
Goldreich, P.: 1965, *Monthly Notices Roy. Astron. Soc.* **130**, 159.
Henrard, J.: 1974, *Celes. Mech.* **10**, 437.
Henrard, J.: 1982a, *Celes. Mech.* **27**, 3.
Henrard, J.: 1982b, 'The Adiabatic Invariant: Its Use in Celestial Mechanics', in V. Szebehely (ed.), *Applications of Modern Dynamics to Celestial Mechanics and Astrodynamics*, D. Reidel Publ. Co., Dordrecht, Holland.
Henrard, J.: 1982c, 'Orbital Evolution of the Galilean Satellities: The Conservative Model', in Ferraz-Mello (ed.), *Proceedings of the Sao Paulo Conference*, D. Reidel Publ. Co., Dordrecht, Holland.
Jupp, A. H.: 1982, *Celes. Mech.* **26**, 413.
Message, P. J.: 1966, 'On Nearly-Commensurable Periods in the Restricted Problem of Three Bodies', *Proc. IAU Symp.* **25**, 197.
Peale, S. J.: 1973, *Reviews of Geophys, and Space Physics* **11**, 767.
Peale, S. J.: 1976, *Annu. Rev. Astron. Astrophys.* **14**, 215.
Peale, S. J., Cassen, P., and Reynolds, R. T.: 1980, *Icarus* **43**, 65.
Poincare, H.: 1902, *Bull. Astron.* **19**, 289.
Schubart, J.: 1966, 'Special Cases of the Restricted Problem of Three Bodies, *Proc. IAU Symp.* **25**, 187.
Yoder, C. F.: 1973, 'On the Establishment and Evolution of Orbit-Orbit Resonances', thesis, Univ. of California, Santa Barbara.
Yoder, C. F.: 1979a, *Celes. Mech.* **19**, 3.
Yoder, C. F. and Peale, S. J.: 1981, *Icarus* **47**, 1.